

## Self-Assembled Lead Chains on Si(100) and Their I - V Characteristics

Zhen-Chao Dong\*, Taro Yakabe, Daisuke Fujita, Stephane Odasso and Hitoshi Nejoj

National Research Institute for Metals, 1-2-1 Sengen, Tsukuba, Ibaraki 305, Japan

Submitted to Journal of Surface Analysis, APF-3

(Received: 9 February 1998; accepted: 26 February 1998)

### Abstract:

The growth of lead on Si(100)2×1 is found by scanning tunneling microscopy to form one-dimensional ad-dimer chains at a coverage far below a monolayer, analogous to the behavior of group-3 elements (Ga, Al, In) on the same surface. However, a different overlay structure appears at the coverage of ~1.5 ML for Pb and three-dimensional Pb islands start to develop with a higher coverage. We investigate the I-V characteristics of Pb structures on Si(100) at these three different coverages. A semiconducting property is observed on both isolated Pb ad-dimer chains at a submonolayer and zigzag Pb chains at ~1.5 ML, while I-V data on 3D Pb islands indicates an expected metallic behavior. The dimerized structure and resultant semiconducting behavior are briefly rationalized by the Peierls distortion mechanism through electron-phonon interaction, that is, the half-filled Pb p<sub>r</sub>-band couples with the lattice so that a gap is opened up just at the Fermi energy.

Transport properties are of primary importance to computation and information processing. An atomic chain, composed of a single row of atoms, is the ultimate limit in the lateral miniaturization of a wire. As nanotechnology is coming of age, there is an increasing demand for scientists to understand and characterize phenomena appearing in atomic scale structures, and further to design and fabricate nanodevices which require atomic scale control. Due to the atomic scale dimension and boundary conditions imposed, the transport behavior of atomic chains is quite different from that in the bulk and could reveal a new intriguing aspect of knowledge and application. Previous scanning tunneling microscopy (STM) studies have established the Stranski-Krastanov growth mode of Group 3- and 4- metals (Al, Ga, In, Sn, or Pb) on Si(100) [1-7], i.e., initial layer growth followed by three-dimensional (3D) island formation. Of particular interest is the initial one-dimensional growth at a coverage of small submonolayers (<<0.5 ML) which has been found to form metal ad-dimer chains perpendicular to the underlying Si dimer rows. The ad-dimer configuration has also been determined to be parallel to the chain direction with each atom three-bonded [8-9]. Our previous I-V data on In/Si(100) [4] have indicated a semiconducting property for such one-dimensional structures, and this behavior can be readily understood in terms of the local chemical bonding of In atoms on the Si(100) surface. Each indium atom (5s<sup>2</sup>5p<sup>1</sup>) saturates

all the unpaired dangling bonds after bonded with two Si atoms and another In atom (yielding an ad-dimer) and leaves no free electrons for metallic conduction. Since each lead atom has one more valence electron than indium, we are curious about the "destiny" of this electron for conduction under the same bonding geometry. Will it be delocalized over the chain, or confined by the Peierls dimerization? In this paper, we report the I-V characteristics of isolated Pb ad-dimer chains on Si(100). To see how conducting properties evolve upon the increase of metal coverages, data on Pb structures at ~1.5 ML and on 3D islands are also presented. The semiconducting property observed on isolated Pb ad-dimer chains is briefly addressed by the Peierls distortion.

All sample preparation and measurements were carried out in an ultrahigh vacuum (UHV) system with facilities for sample heating and cooling, metal deposition, and characterization by scanning tunneling microscopy (JEOL JSTM-4500 XT). The base pressure of the system is less than 2×10<sup>-10</sup> Torr. Samples (1×6.8×0.25 mm<sup>3</sup>) were cut from a commercial polished Si(100) wafer (n-type, 1-10 Ω·cm) with a misorientation less than 0.7°, and ultrasonically cleaned in acetone before introduction into the UHV chamber. Atomically flat Si(100)2×1 surfaces were obtained after outgassing at ~450°C for ~12h, flashing up to ~1250°C (estimated by an infrared pyrometer) for total ~1 min, and finally, slow cooling from ~950°C to room

temperature. Substrate heating was achieved by passing a current directly through the sample. The base pressure was kept below  $5 \times 10^{-9}$  Torr during the above flashing procedure. Lead metal (99.99%) was evaporated from a heated tungsten basket onto the substrate kept at room temperature. The coverages were controlled by adjusting both the power applied to the W coil and the deposition time. Accurate determination of the local coverage was made by counting the density of Pb ad-dimers observed in the STM images for coverages less than 0.5 ML. All images were taken in the constant current topographic (CCT) mode. Low-temperature data on 3D Pb islands were obtained after the deposited sample was cooled down to 80 K by liquid nitrogen. Tips used for imaging and local I-V measurements were prepared by electrochemical etching of a W wire in a 2-N NaOH solution, followed by in-situ cleaning in vacuum by heating the tip apex up to  $\sim 1000^\circ\text{C}$ .

Figure 1 shows three topographs at different Pb coverages on Si(100) [6-7]. Each bright protrusion in Figure 1a ( $(32 \text{ nm})^2$ , 0.1 ML, sample bias = -1.9 V, tunneling current = 0.5 nA, 296K) corresponds to a Pb ad-dimer and is clearly distinguishable from the underlying Si dimer rows (filled states). The one-dimensional growth of Pb on Si(100) is evident. As the coverage is increased to  $\sim 1.5$  ML, an overlayer structure similar to the reported  $c(4 \times 4)$  [6-7] was observed in Figure 1b ( $(60 \text{ nm})^2$ ,  $\sim 1.5$  ML, -2.1 V, 1.0 nA, 295K). However, the exact reconstruction of this surface remains to be identified since the  $c(4 \times 4)$ -Pb consists of two orthogonal domains, and the zigzag rows are oriented at  $45^\circ$  to the step edges. Our image does not show clearly this kind of orientation but instead has chains running in many different directions (mixed with the  $2 \times 1$ -Pb phase), possibly a result of high defect densities on the original Si(100) surface or an insufficient metal coverage. As

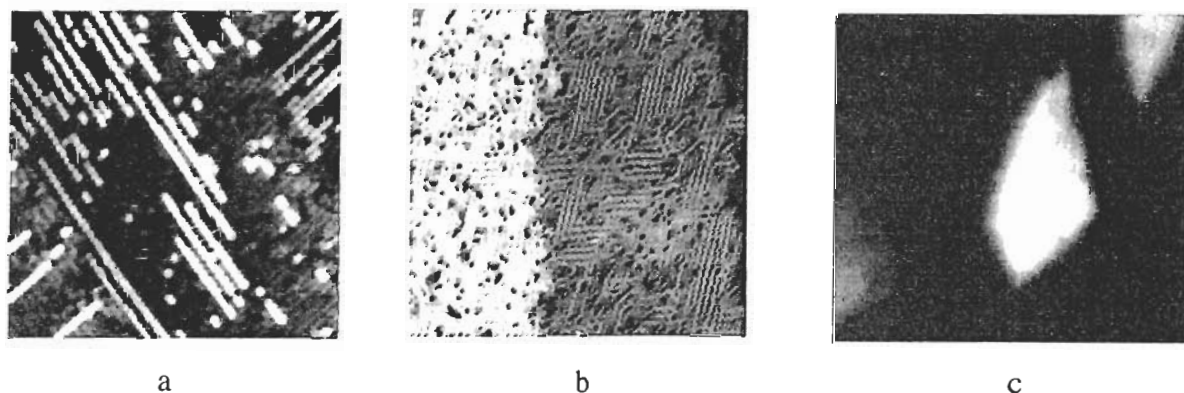


Fig.1 STM topographs of Pb on Si(100)  $2 \times 1$ , (a) isolated Pb ad-dimer chains,  $32 \times 32 \text{ nm}^2$ , 0.1 ML, -1.9V, 0.5nA, 295K; (b) zigzag Pb chains on a rough  $c(4 \times 4)$ ,  $60 \times 60 \text{ nm}^2$ ,  $\sim 1.5$  ML, -2.1V, 1.0nA, 295K; (c) 3D Pb islands,  $300 \times 300 \text{ nm}^2$ ,  $>2$  ML, +1.8V, 0.5nA, 80 K.

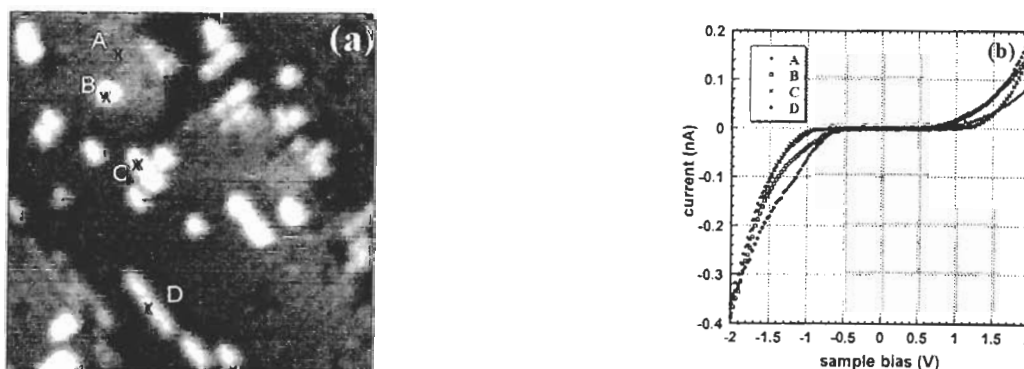


Fig.2 (a) A topograph of Pb on Si(100)  $2 \times 1$  at a coverage of 0.05 ML showing different lengths of Pb ad-dimer chains ( $20 \times 20 \text{ nm}^2$ , -2.3V, 0.5nA); (b) I-V data measured at the specific locations marked by the crosses in (a).

the Pb coverage continue to increase ( $> 2$  ML), 3D islands start to form on top of the two-dimensional Pb layer, as shown in the empty-state image of Figure 1c ( $(300 \text{ nm})^2$ , +1.8 V, 0.5 nA, 80 K). No regular-shaped islands were observed during this experiment. Figure 1 reproduces the Stranski-Krastanov growth mode of Pb on Si(100). The detail of Pb overlayer structures is not our primary concern and is not given here, but is nicely described in the work of Itoh, et al. [6] and Li, et al. [7].

The I-V data measurements on isolated Pb ad-dimer chains were carried out on a  $(20 \text{ nm})^2$  surface with a 0.05 ML coverage of Pb, as shown in Figure 2a, which was taken at room temperature with  $-2.3 \text{ V}$  sample bias (filled states) and 0.5 nA current. Typical I-V characteristics are displayed in Figure 2b with measurements performed at different specific locations on the surface marked in Figure 2a by crosses: A on a bare Si(100) surface, B on top of a double-ad-dimer chain, C on top of a five-ad-dimer chain, and D on top of a seven-ad-dimer chain, respectively. The observed surface-state bandgap of  $\sim 1 \text{ eV}$  on the bare Si(100) is consistent with previous reports by tunneling spectroscopy [10] and photoemission and inverse photoemission studies [11]. Similarly, data on top of Pb ad-dimer chains shows a surface-state bandgap of  $1.0 - 1.5 \text{ eV}$ , although we have not been able to figure out the chain-length dependence. The common feature among the four, the existence of a surface-

state bandgap, implies a semiconducting behavior on these surface structures. And the localized electron picture in the case of Pb chains can be rationalized by the Peierls pairing mechanism (below).

Typical I-V data on zigzag Pb chains at  $\sim 1.5 \text{ ML}$  (Figure 1b) are shown in Figure 3a, whereas those on 3D Pb islands (Figure 1c) are displayed in Figure 3b. It is quite surprising that the two-dimensional Pb overlayers composed of three Pb sub-layers appear not conducting as the I-V curves again exhibit a surface-state bandgap of  $\sim 0.7 \text{ eV}$ , although the bandgap appears smaller than the isolated Pb ad-dimer chains. The three curves in the figure correspond to different initial regulated tip heights. A larger regulated current signifies a smaller tip-sample gap distance and thus a larger tunneling current for the same bias condition. The semiconducting behavior is still possibly related to the Peierls distortion mechanism, but the  $c(4 \times 4)$  structure is complicated and the distortion mechanism will not be discussed here. On the other hand, metallic conduction is reasonably observed on the 3D Pb islands since there is no surface-state bandgap in the I-V curves (Figure 3b). This is consistent with the photoemission studies on Pb/Si(100) by Le Lay, et al. [12] in which they reported the metallization upon the onset of 3D nucleation and the development of metallic Pb clusters. It is worthy to note that the asymmetrical features of I-V curves in

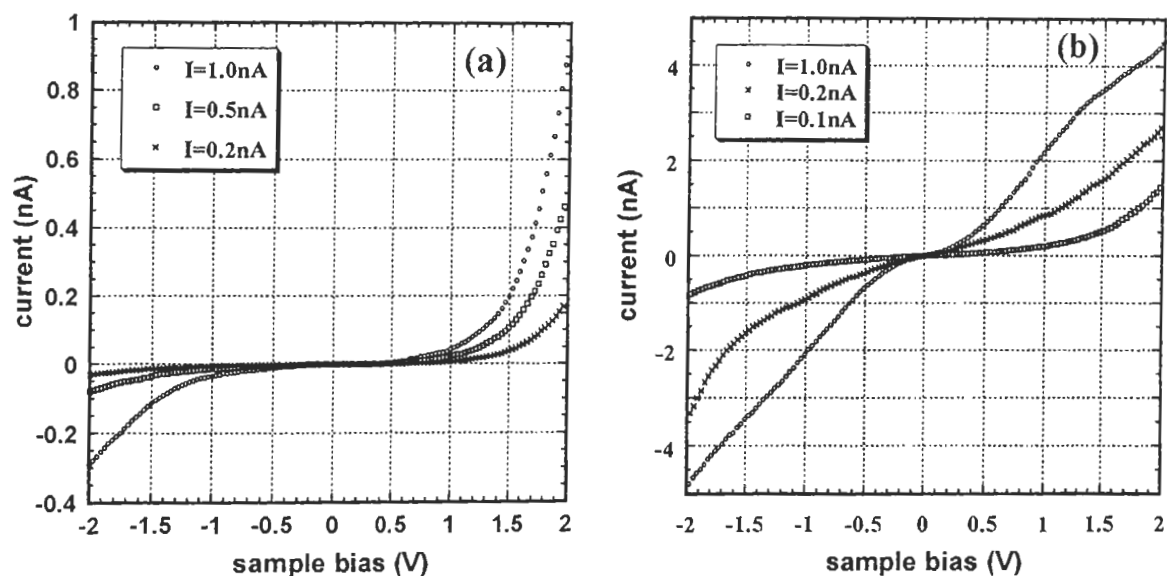
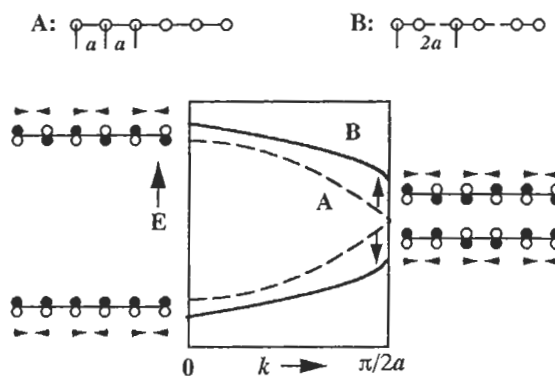


Fig.3 I-V data acquired on top of (a) zigzag Pb chains at  $\sim 1.5 \text{ ML}$ ; (b) 3D Pb islands at  $> 2 \text{ ML}$ . Different curves correspond to different initial regulated tip heights.

Figure 2b and Figure 3 are a combined result of tip condition and sample doping. When an experiment involved the lead deposition, we occasionally observed very asymmetrical I-V curves and obtained images of different quality for different bias polarities. These features are probably caused by a contaminated W-tip which picked up a Pb atom or cluster during scanning, but the effect of a Pb-contaminated tip on tunneling remains to be understood.

The observed Pb ad-dimer chain structure and its semiconducting property on Si(100) agrees well with the spirit of the Peierls pairing mechanism. According to Peierls [13], an equidistant one-dimensional metal chain can never be stable, because the electron-phonon coupling will animate dimerization or bond-alternation, and the atomic rearrangement is exactly such that an energy gap is opened up at the Fermi level (in other words, the Fermi surface is nested). Whether a Peierls distorted structure will occur or not depends on both the energy lowering from the distortion and the strain caused by the binding between Pb and the surface. Each Pb atoms form three (-bonds with neighboring atoms while there is still one perpendicular p-orbital available for  $\pi$ -type bonding. The observed dimerized structure suggests that the decrease in electron energy surpasses the increase in lattice (strain) energy. Figure 4 illustrates schematically the modification of band structures for an atomic chain upon a Peierls dimerization. Model A represents a hypothetical equidistant linear chain ( $a = 3.84 \text{ \AA}$ ). The band (dashed lines) is typically folded when the periodicity is artificially doubled. Model B is the dimerized structure observed in the experiments. Each black-white dumbbell represents an unpaired p-orbital that is oriented perpendicular to the chain direction. The energy lowering upon pairing is clearly visible from the p-orbital interactions. At the bottom (all p-orbital in-phase) and top (all p-orbital out-of-phase) of the bands, no substantial changes occur. However, at  $k = \pi/2a$ , the pairing has a dramatic effect. The original double degeneracy at the Fermi level is broken with the lower in-phase-pairing band going down and the upper out-of-phase-pairing band raising up. The total energy is thus reduced since only the lower band is filled. It is also evident that the net stabilization of a system through the Peierls distortion is maximal for the half-filled band because a gap is opened up



**Fig.4** Schematic diagram of the Peierls distortion of a Pb atomic chain on Si(100). A: a hypothetical equidistant linear chain, B: a Peierls distorted dimer chain. The half-filling of the p-band for the model A leads to an electron-phonon coupling that opens up a gap at the zone edge. Each black-white dumbbell represents an unpaired p orbital oriented perpendicular to the chain.

right at the Fermi energy. In other words, the half-filling leads to an electron-phonon coupling that introduces a gap just at the Fermi level.

In summary, we have investigated the I-V characteristics of Pb structures on Si(100) at three different coverages. A semiconducting property is observed on both isolated Pb ad-dimer chains at a submonolayer coverage and zigzag Pb chains at  $\sim 1.5 \text{ ML}$ . Pb deposition with a higher coverage results in the growth of 3D islands and our I-V data indicates a metallic behavior, suggesting the formation of metallic Pb clusters. The dimerized structure and resultant semiconducting behavior are briefly rationalized by the Peierls distortion mechanism through the electron-phonon coupling. Approaches to rendering these one-dimensional structures metallic include electron doping into an empty band or artificial structuring of the atomic chains [14-15], increasing the temperature and pressure, or alternatively, the fabrication of larger-sized cluster chains or molecular wires rather than atomic lines [16-18]. Further research is underway.

#### Acknowledgments

This work is supported by the Science Promotion and Coordination Budget from the Science and Technology Agency of Japan.

## References

1. Nogami, J., Baski, A. A. and Quate, C. F., *Phys. Rev. B* **44** (1991) 1415.
2. Nogami, J., Park, S.-I. and Quate, C. F., *Appl. Phys. Lett.* **53** (1988) 2086.
3. A. A. Baski, J. Nogami and C. F. Quate: *Phys. Rev. B* **43** (1991) 9316.
4. Z.-C. Dong, T. Yakabe, D. Fujita, Q. D. Jiang and H. Nejoh, *Surf. Sci.* **380** (1997) 23.
5. Baski, A. A., Nogami, J. and Quate, C. F., *Phys. Rev. B* **50** (1994) 10834.
6. H. Itoh, H. Tanabe, D. Winau, A. K. Schmid and T. Ichinokawa, *J. Vac. Sci. Technol. B* **12** (1994) 2086.
7. L. Li, C. Koziol, K. Wurm, Y. Hong, E. Bauer and I. S. T. Tsong, *Phys. Rev. B* **50** (1994) 10834.
8. J. E. Northrup, M. C. Schabel, C. J. Karlsson and R. I. G. Uhrberg: *Phys. Rev. B* **44** (1991) 13799.
9. G. Brocks, P. J. Kelly and R. Car: *Phys. Rev. Lett.* **70** (1993) 2786.
10. R. J. Hamers and U. K. Kohler, *J. Vac. Sci. Technol. A* **7** (1989) 2854.
11. F. J. Himpsel and Th. Fauster, *J. Vac. Sci. Technol. A* **2** (1984) 815.
12. G. Le Lay, K. Hricovini and J. E. Bonnet, *Phys. Rev. B* **39** (1989) 3927.
13. R. E. Peierls, *Quantum Theory of Solids*, 1st ed. (Oxford University Press, Oxford, England, 1955), p.108.
14. T. Hashizume, S. Heike, M. Lutwyche, S. Watanabe, K. Nakajima, T. Nishi and Y. Wada: *Jpn. J. Appl. Phys.* **35** (1996) L1085.
15. Z.-C. Dong, T. Yakabe, D. Fujita, T. Ohgi, D. Rogers and H. Nejoh, to be published in *Jpn. J. Appl. Phys.* 1998 (March issue).
16. A. Thess, et al.: *Science* **273** (1996) 483.
17. S. Iijima: *Nature* **354** (1991) 56.
18. C.-G. Wu and T. Bein: *Science* **266** (1994) 1013.

\* Corresponding author: Fax: +81-0298-59-2701,  
Email: dzc@nrim.go.jp,